Morphology and magnetic properties of W-capped Co nanoparticles

A. I. Figueroa, J. Bartolomé, L. M. García, F. Bartolomé, C. Magén et al.

Citation: J. Appl. Phys. **107**, 09B508 (2010); doi: 10.1063/1.3368725
View online: http://dx.doi.org/10.1063/1.3368725
View Table of Contents: http://jap.aip.org/resource/1/JAPIAU/v107/i9
Published by the American Institute of Physics.

Morphology and magnetic properties of W-capped Co nanoparticles

A. I. Figueroa,[1,a)] J. Bartolomé,[1] L. M. García,[1] F. Bartolomé,[1] C. Magén,[2] A. Ibarra,[2] L. Ruiz,[3] J. M. González-Calbet,[3] F. Petroff,[4] and C. Deranlot[4]
[1]*Departamento de Física de la Materia Condensada, Instituto de Ciencia de Materiales de Aragón, CSIC-Universidad de Zaragoza, E-50009 Zaragoza, Spain*
[2]*Departamento de Física de la Materia Condensada, Instituto de Nanociencia de Aragón-ARAID, Universidad de Zaragoza, Zaragoza, Spain*
[3]*Departamento de Química Inorgánica, Universidad Complutense de Madrid, E-28040 Madrid, Spain*
[4]*Unité Mixte de Physique CNRS/Thales and Université Paris-Sud, Orsay, France*

(Presented 19 January 2010; received 30 October 2009; accepted 2 March 2010; published online 21 April 2010)

Co–W nanoparticles formed by sequential sputtering of Co on amorphous alumina substrate and subsequent W capping are studied by high resolution and by scanning transmission electron microscopies, and by superconducting quantum interference device magnetometry. The analysis is focused on W nominal thickness dependence. Results suggest the formation of amorphous Co–W alloy nanoparticles, whose magnetic moment per Co atom is systematically reduced as the nominal thickness of W capping layer increases. The Co–W nanoparticles show superparamagnetic behavior. The activation energy for moment reversal and the effective anisotropy are obtained. © *2010 American Institute of Physics*. [doi:10.1063/1.3368725]

It has been recently shown that the magnetic properties of nanoparticles are modified by capping with different metals. To study this effect, the system of choice are Co nanoparticles deposited on an amorphous alumina substrate since they form nanoclusters evenly distributed on the substrate for nominal thickness of deposited Co, t_{Co}, below a certain threshold.[1] In previous works, we have studied the effect of noble metals such as Cu, Ag, and Au on Co nanoparticles predeposited on alumina.[2,3] The capping noble metal does not diffuse on Co, so that the Co particle retains its integrity as a nearly spherical particle. We have demonstrated that there is an enhancement of surface anisotropy with respect to the uncapped Co nanoparticles following that trend.

In this work, a W metal cap has been chosen because of the known affinity to produce Co–W alloys, on one hand, and the tendency of these alloys to become amorphous.[4,5] Moreover, the W metal has a less than half filled 5d band, so a drastic contrast in the magnetic behavior of the W–capped Co nanoparticles could be expected. For example, W alloyed with Co is known to suppress the latter magnetic moment when forming Co–W alloys.[4] This method of capping with W, therefore, could tailor the magnetic moment per Co atom controlling the amount of W sputtered on the Co predeposited nanoparticle.

Studied samples were prepared by sequential sputtering deposition of Al_2O_3, Co, and W on a Si substrate, following the same procedure as it is described in previous works on metal capped Co nanoparticles.[3] Cobalt cluster films are formed by aggregation of metal atoms sputter deposited on amorphous alumina and subsequently capped with a W layer. This process is done once to obtain a monolayer and repeated 25 times to get a multilayer system, following the formula $Al_2O_3/(Al_2O_3/Co/W)_{25}/Al_2O_3$. In this paper, we present a W-thickness dependence study, for samples with t_{Co} fixed at 0.7 nm and nominal thickness of W, t_W, varied between 0.6, 1.5, and 4.5 nm.

High-resolution transmission electron microscopy (HRTEM) observation was performed in cross section configuration on all three samples and in plan view configurations on samples with t_W=0.6 and 1.5 nm. High angle annular dark field (HAADF) scanning transmission electro microscopy (STEM) observation was carried out on these last two samples. For t_w=0.6 nm [Fig. 1(a)] and t_w=1.5 nm samples,

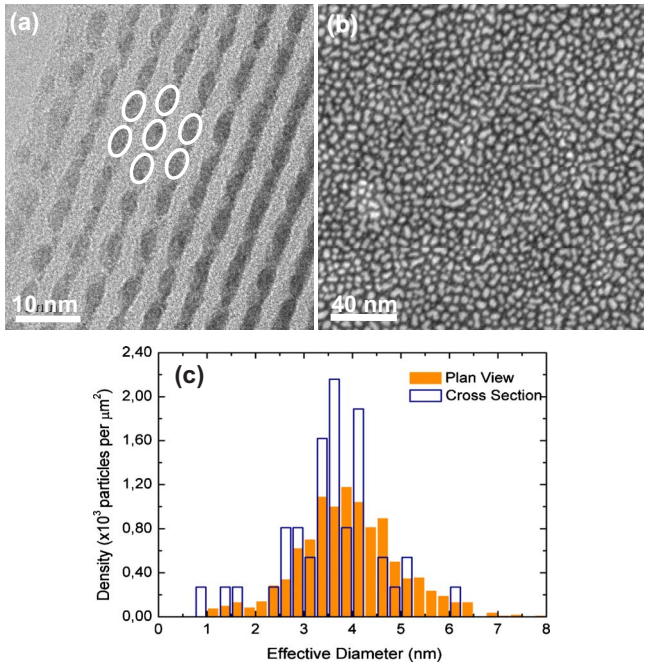

FIG. 1. (Color online) Morphology study of sample with t_W=0.6 nm. (a) HRTEM image in cross section configuration. (b) HAADF STEM image in plan view configuration. (c) Size distribution of both configurations.

[a)]Electronic mail: figueroa@unizar.es.

TABLE I. Average particle diameter $\langle D_{\text{eff}} \rangle$, distribution width, σ, interparticle distance, d, and density of particles in the layer, N_S, obtained from digital analysis of TEM images.

Cross section				Plan view			
t_W (nm)	$\langle D_{\text{eff}} \rangle$ (nm)	σ (nm)	d (nm)	$\langle D_{\text{eff}} \rangle$ (nm)	σ (nm)	d (nm)	N_S ($\times 10^{-2}$ nm^2)
0.6	3.6(1)	0.4(2)	5.8(5)	3.87(4)	0.82(6)	5.3(5)	3.2(1)
1.5	3.9(1)	0.9(5)	6.6(7)	4.23(6)	1.0(1)	5.6(9)	3.5(1)

HTREM and energy dispersive x-ray analysis indicate that light gray layers correspond to alumina and darker layers to metal (Co and W), both amorphous. These layers exhibit a washboard cross sectional shape in both samples where it is possible to identify amorphous particles with elongated shape arranged in a hexagonal fashion, as marked in Fig. 1(a), across the layers. This is in stark contrast to the fcc Co well crystallized nanoparticles observed when capping with a noble metal.[3]

High contrast obtained in plan view STEM images [Fig. 1(b)] allows easier identification of the particles than in HRTEM images due to the huge Z contrast between the heavy metal particles and the light oxide matrix. Images obtained are comparable to those of similar systems of metallic nanoparticles embedded in insulator matrices.[6] HAADF STEM images reveal that particles in sample with $t_W = 1.5$ nm are bigger and more closely packed than particles in sample with $t_W = 0.6$ nm.

Size distributions for samples with $t_W = 0.6$ [Fig. 1(c)] and 1.5 nm were made by digital processing of the images taken, for both cross section and plan view configurations. Even though these two distributions seem to be centered at the same mean area, there is a slight difference between both values. Area projection for plan view is larger than the one for cross section in both samples with $t_W = 0.6$ nm and 1.5 nm, which means that particles tend to have an oblate shape.

The values obtained from this analysis are shown in Table I. Effective diameter, $\langle D_{\text{eff}} \rangle$, is obtained from the assumption that particles have elliptic in-plane and out-of-plane projection shape, with short axis a and long axis b, so that $D_{\text{eff}} = \sqrt{ab}$. Interparticle distance, d, and surface density of particles, N_S, expressed as number of particles per nm^2, are almost equal for both samples, which means that particles are spatially distributed on each layer in the same way for $t_W = 0.6$ nm and for $t_W = 1.5$ nm samples. Cross section values have a higher error since they were obtained from poor contrast HRTEM images, so particles identification was less precise than in the plan view case.

A magnetometry study was performed on the same samples by $\chi_{\text{dc}}(T)$, $\chi_{\text{ac}}(T)$ and $M(H)$ measurements in a commercial superconducting quantum interference device magnetometer. $\chi_{\text{dc}}(T)$ was measured after cooling the sample in zero field (ZFC) and in the presence of a field (FC). Temperature was varied between 5 and 150 K, and a 200 Oe field was applied (Fig. 2). These curves show that W-capped Co nanoparticles have a superparamagnetic behavior, similar to those uncapped and Cu-, Ag-, and Au-capped Co nanoparticles.[2,7] The $M(H)$ curves were identical when measured with the field parallel and perpendicular to the sample plate, therefore the particle anisotropy axes are randomly distributed and the demagnetization factor plays no role in the present case. At high temperatures, all curves follow the Curie–Weiss law $\chi_{\text{eq}} = C/(T-\theta)$. At lower temperatures, FC and ZFC for each sample separate and the ZFC curve shows a maximum at a blocking temperature, T_B. Values of T_B for W capped Co nanoparticles are lower than those of the uncapped ones. T_B is also reduced as the W capping layer gets thicker. Values for T_B obtained from this analysis are shown in Table II.

$M(H)$ measurements plotted in Fig. 3 were performed at $T \approx 3T_B$ for same samples shown in Fig. 2. Applied fields were varied up to 50 kOe. It is evident that saturation magnetization, M_S, per Co atom deposited in the sample decreases as the W capping layer thickness increases for a constant $t_{\text{Co}} = 0.7$ nm.

Tungsten is forming an amorphous alloy with the Co atoms and is strongly reducing the magnetic moment on the Co atoms. This reduction may be due to combined effect of charge transfer, hybridization and environmental effects, as it is described in Ref. 4. According to this author, when the number of Co first neighbors is higher than 3, Co atoms carry their full moment of $1.7\mu_B/at$, as in uncapped Co nanoparticles.[2] If the Co atom has less Co atoms as first neighbors, e.g., 2 or 3 Co atoms, its magnetic moment decreases to about $0.5\mu_B/at$. The latter value is well in agreement with the moments found for Co atoms in the samples studied in this work.

A simple method to determine the magnetic moment per particle consists in dividing the saturation magnetization by the number of particles N_S, both, per unit surface, as determined from the STEM images. Since W has a negligible induced moment, the magnetization is supported by the Co

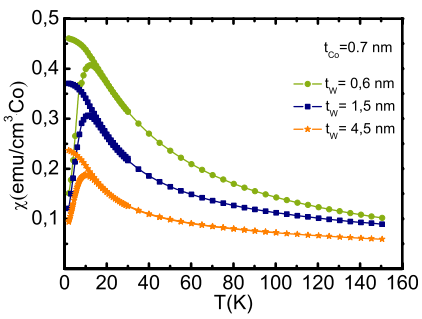

FIG. 2. (Color online) DC susceptibility curves for samples with $t_{\text{Co}} = 0.7$ nm, and different W capping thicknesses, $t_W = 0.6$, 1.5, and 4.5 nm.

TABLE II. Summary of the parameters deduced from the magnetic measurements on Co–W Nanoparticles (t_{Co}=0.7 nm).

t_W (nm)	T_B (K)	θ (K)	M_S (μ_B/Co)	m_{part} ($\times 10^{-3}\mu_B$/part.)	$\langle D_{mag}\rangle$ (nm)	σ_{mag} (nm)	$\langle U\rangle$ (K)	K_{eff} ($\times 10^{-6}$ erg/cm^3)
0.6	9.97(2)	7.3(2)	0.52(1)	1.03(1)	3.4(2)	0.25(5)	270(10)	1.43(5)
1.5	9.52(4)	4.5(1)	0.46(1)	0.84(1)	3.2(2)	0.32(5)	220(4)	1.20(7)
4.5	9.00(9)	5.5(2)	0.30(1)	0.57(1)	3.4(6)	0.38(5)	200(10)	1.0(1)

atoms. The average amount of Co atoms per particle is also easily determined by the ratio of deposited Co and number of particles, per unit surface. The resulting moment per Co atom (Table II) decreases with increasing W cap thickness, and ranges between 0.52 and 0.30, for t_W=0.6 and 4.5, respectively. Thus, the reduction in Co moment expected for Co–W alloying[4] is duly verified. In fact, an average alloy composition may be proposed by comparing the M_S values to those measured for bulk alloys. The W concentration that explains the reduction in magnetic moment ranges from 18.2, 18.8, to 20.3 at. % with t_W=0.6, 1.5, and 4.5 nm, respectively.[5]

The $M(H)$ curves have been fitted to a Langevin function, averaged with a Gaussian distribution of particle size, under the assumption that the Co moment in the particle is that derived in the precedent paragraph. Considering the Co–W composition deduced in the previous paragraph for each particle t_W, this analysis yields to the effective magnetic core diameters $\langle D_{mag}\rangle$ and distribution width σ given in Table II. These parameters are verified by checking the prediction of the $1/\chi(T)$ curve in the superparamagnetic temperature regime for particles of that diameter and size distribution.

$\chi_{ac}(T)$ was measured by applying an ac field of 4.0 Oe to the sample with frequency $\omega/2\pi$ in between 1.0 and 480 Hz. Analysis of the imaginary part of $\chi_{ac}(T)$ allowed the determination of the activation energy, $\langle U\rangle$, which corresponds to the energy barrier for the thermally activated magnetization reversal. The rate at which magnetic moment of the particles flip is determined by the anisotropy K_{eff}, so that we write $\langle U\rangle = K_{eff}V$, with $\langle V\rangle$ being the particle magnetic volume. The relaxation time is given by Arrhenius' law $\tau = \tau_0 \exp(\langle U\rangle/k_BT)$. Variation of T_B with frequency follows Arrhenius' law, as well, and provides a direct measure of the anisotropy strength. The values of $\langle U\rangle$ and K_{eff} found for W-capped Co nanoparticles are given in Table II.

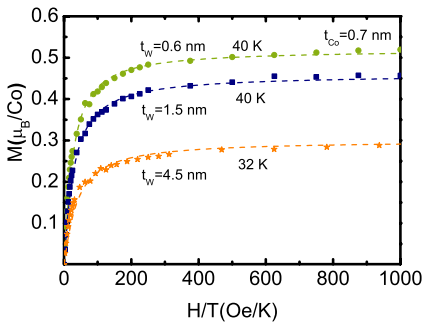

FIG. 3. (Color online) Magnetization curves for samples with t_{Co}=0.7 nm, and different W capping thickness, t_W=0.6, 1.5, and 4.5 nm, measured at 40, 40, and 32 K, respectively. The dashed lines are fitted Langevin curves with $\langle D_{mag}\rangle$ and σ parameters given in Table II.

An interesting conclusion is derived from this analysis, namely, the average particle size and size distribution derived from direct HAADF, STEM, and HRTEM observation $\langle D_{eff}\rangle$ is a bit larger than the effective magnetic particle $\langle D_{mag}\rangle$ and σ. The not alloyed excess W surrounds the magnetic particle core and tends to fill the interparticle space [Fig. 1(a)].

The effective anisotropy $K_{eff}=\langle U\rangle/[\pi\langle D_{mag}\rangle/6]$, that is, assuming that the magnetic moment is just supported by the Co–W magnetic alloy core, decreases with increasing t_W (Table II). Shape anisotropy cannot explain the $K_{eff} \approx 10^6$ erg/cm^3 found since it is two orders of magnitude smaller for our oblate particles. Stress anisotropy is also one order of magnitude smaller.[8] Since there is no definite interface between the core alloy and the excess W, surface is not likely to generate anisotropy. Therefore, we think that texturing of the alloy within the particle may be causing the found K_{eff}.

Concluding, the Co preformed nanoparticles attract the W during the deposition forming Co–W amorphous alloy particles with a ratio of W in the range of 18.2–20.3 at. %. Any excess, not alloyed W tends to fill the interparticle spaces, but being not magnetic, play no role in the magnetic response. The description in terms of noninteracting clusters is supported by (a) the reduction in the magnetic moment per particle, which therefore reduced dipolar interactions with respect to the uncapped particles,[7] and (b) the irrelevance of Ruderman–Kittel–Kasuya–Yosida interaction, which would cause an increase in T_B instead of the observed reduction.[2]

The financial support of MAT08/1077 is acknowledged. A. I. Figueroa acknowledges a JAE-Predoc grant.

[1] D. Babonneau, F. Petroff, J. Maurice, F. Fettar, A. Vaures, and A. Naudons, Appl. Phys. Lett. **76**, 2892 (2000).
[2] F. Luis, F. Bartolomé, F. Petroff, J. Bartolomé, L. M. García, C. Deranlot, H. Jaffrès, M. J. Martínez, P. Bencok, F. Wilhelm, A. Rogalev, and N. Brookes, Europhys. Lett. **76**, 142 (2006).
[3] J. Bartolomé, L. M. García, F. Bartolomé, F. Luis, R. López-Ruiz, F. Petroff, C. Deranlot, F. Wilhelm, A. Rogalev, P. Bencok, N. Brookes, L. Ruiz, and J. González-Calbet, Phys. Rev. B **77**, 184420 (2008).
[4] K. H. J. Buschow, J. Appl. Phys. **54**, 2578 (1983).
[5] M. Naoe, H. Kazama, Y. Hoshi, and S. Yamanaka, J. Appl. Phys. **53**, 7846 (1982).
[6] D. Babonneau, D. Lantiat, S. Camelio, J. Toudert, L. Simonot, F. Pailloux, M.-F. Denanot, and T. Girardeau, Eur. Phys. J.: Appl. Phys. **44**, 3 (2008).
[7] F. Luis, J. Torres, L. M. García, J. Bartolomé, J. Stankiewicz, F. Petroff, F. Fettar, J. Maurice, and A. Vaures, Phys. Rev. B **65**, 094409 (2002).
[8] P. Hansen, in *Handbook of Magnetic Materials 6*, edited by K. H. J. Buschow (Elsevier Science, Amsterdam, 1991), p. 289.